2018 European Control Conference (ECC)
June 12-15, 2018. Limassol, Cyprus

Dual Dynamic Programming for Nonlinear Control Problems over Long Horizons

Benjamin Flamm, Annika Eichler, Joseph Warrington, John Lygeros

Abstract— **We propose a split-horizon decomposition scheme to compute approximate solutions to discrete-time nonlinear control problems over long horizons. The proposed optimization scheme combines a short horizon using an accurate, complex system model, with a longer horizon using a simplified model. A piecewise-linear terminal value function found using dual dynamic programming is introduced to couple the short and long horizons of the approximate problem. We introduce a method that iterates between solving each sub-problem, and prove this converges to the optimum of the combined problem. This approach allows solutions over longer horizons than would be tractable for the full nonlinear program, with better modeling accuracy than a convex relaxation of the entire horizon. The method is applied to profit-maximizing seasonal control strategies on the Swiss day-ahead spot electricity market for an electrolyzer/fuel cell system with hydrogen storage. The problem is formulated as a mixed integer quadratically-constrained program, with per-period fixed costs and quadratic energy conversion efficiencies. We show that our method, when applied in a receding horizon manner, achieves near-optimal solutions over horizons of multiple months, using short-term exact horizons of less than three days.**

I. Introduction

Optimal control of nonlinear systems over a long time horizon is inherently difficult, due to the large number of decision variables and nonconvexity of the problem. For this reason, accurate system models are often replaced by approximations in order to be solvable over the desired time horizon. A primary application area for control over long time horizons is the optimization of seasonal storage such as hydropower, in which reservoirs are charged or discharged according to forecast prices and electricity demand. The hydro optimization literature is rich with examples of how to optimally operate such systems over long horizons.

Dual dynamic programming (DDP), also known as multistage Benders decomposition, was introduced as a method for seasonal hydro storage scheduling in [1], but has since been used primarily for solving linear approximations of these problems. In the class of problems we consider in this paper, planning difficulties stem from the nonlinear models that characterize the devices. Since DDP cannot solve problems with a nonconvex value function, convex approximations and relaxations of the model are required to use DDP. In [2], the authors introduce piecewise-linear approximations of nonlinear cost functions. In [3], Lagrangian relaxation is employed to generate locally-valid value functions. In [4], McCormick envelopes are used to generate a convex approximation of a bilinear cost function. In [2]-[4], model complexity is reduced throughout the entire horizon.

Long-term decision problems can also be split into multiple stages using DDP, as done for hydro system operation over linked markets with distinct dynamics in [5]. The value for the second stage is calculated using a version of DDP, and added to the cost function for the first stage. Multistage models which separate problem stages based on reservoir size are introduced in [6]. The value function for large storage reservoirs is determined via DDP, and used as a water value for small balancing reservoirs. Due to vast differences in reservoir sizes, the dynamics of the first and second stages are assumed to be independent.

Other approaches to multi-stage mixed integer programs have considered topics such as the convergence of branch-and-bound algorithms [7]. However, these approaches remain intractable over the long periods in which we are interested.

With the application to long-term energy storage in mind, we propose a method for calculating an approximate solution to a nonlinear control problem with a long horizon. We split the full horizon into short- and long-term parts, with high model accuracy in the short term, and reduced model accuracy in the long term. In the second part of the horizon, we relax binary variables and generate linear approximations for nonlinear functions, as in [8]. Unlike previous approaches [2]-[4], we use the exact nonlinear model in the first part. We assume that the solution of the nonlinear problem is tractable over the first part of the horizon.

To link the two parts of the horizon, we establish an appropriate future value for the system state at the end of the short term. Adopting the language of model predictive control (MPC), we refer to this value as the “terminal cost” [9]. Note that the terminology is often application-specific; in pumped hydro storage optimization literature, it is referred to as the “water value.” By Bellman’s principle of optimality, all information concerning future costs under optimal long-term behavior can be encapsulated in a value function at the end of the first part of the horizon [10].

The two parts of the horizon are coupled using a terminal cost based on DDP, which bounds the value of the terminal state of the short horizon by a piecewise-affine function of the state. We show that when this method is applied in a receding horizon manner, we can solve otherwise intractable long-term problems. In the given numerical example, this is done to near-optimality. To our knowledge, DDP has not been applied to multistage nonlinear control problems before.

This work was supported by the Swiss Competence Center for Energy Research FEEB&D project, ETH Zürich Energy Science Center IMES project, and Nano-tera.ch HeatReserves project.

The authors are with the Automatic Control Laboratory of ETH Zürich, Physikstrasse 3, 8092 Zürich, Switzerland. {flammb, eichlean, warrington, lygeros}@control.ee.ethz.ch

As an application for this method, we consider the profit-maximizing operation of a large-scale power-to-gas hydrogen seasonal storage device exposed to spot electricity prices. As electricity prices and energy demand often follow a yearly cycle, the optimal controller must take into account long-term trends. This paper uses a model of a custom proton electrolyte membrane (PEM) electrolyzer/fuel cell system with attached hydrogen and oxygen storage, currently being developed by Paul Scherrer Institut in Villigen, Switzerland.

In Section II, a mixed integer nonlinear program (MINLP) is formulated, and a split-horizon approximation of the MINLP is presented. To connect the two parts of the approximate problem, a terminal cost based on DDP is introduced. In Section III, an algorithm is proposed that solves the two-part approximation to optimality. Convergence of this method is proven. In Section IV, an example power-to-gas energy storage system is considered. Section V presents the simulation results for this system, illustrating the computational benefit and near-optimality of the split-horizon approximation for this particular application. Finally, Section VI concludes and provides suggestions for future work.

II. Problem Setting and Background

A. Cost Minimization Problem

We consider a generic discrete-time optimal control problem for a system with dynamics f_t, input and state constraints defined by membership in the compact set $\mathcal{Z}_t$, and cost function g_t over a horizon of length N. The input is denoted by $u = (u_0, \ldots, u_{N-1})$, while the state is $x = (x_0, \ldots, x_N)$.

For a given timestep t, we have $u_t \in \mathbb{R}^{l_t^{(1)}} \times \{0,1\}^{l_t^{(2)}}$, with $l_t^{(1)}$ and $l_t^{(2)}$ the number of continuous and binary variables in the input. Similarly, $x_t \in \mathbb{R}^{m_t^{(1)}} \times \{0,1\}^{m_t^{(2)}}$, with $m_t^{(1)}$ and $m_t^{(2)}$ the number of continuous and binary variables in the state. The optimal inputs for a given horizon are determined by solving the mixed integer nonlinear program (MINLP)

$$\min_{x,u} \sum_{t=0}^{N-1} g_t(x_t, u_t) + g_N(x_N) \tag{1a}$$

$$\text{s.t.} \quad x_{t+1} = f_t(x_t, u_t), \qquad t = 0, \ldots, N-1 \tag{1b}$$

$$(u_t, x_t) \in \mathcal{Z}_t, \qquad t = 0, \ldots, N-1 \tag{1c}$$

$$x_0 \text{ given,} \tag{1d}$$

where $f_t(x_t, u_t)$ and $g_t(x_t, u_t)$ are nonlinear functions. The dynamics, costs, and constraints can all be time-varying.

Inspired by the seasonal energy storage planning setting considered below, we wish to solve this problem over horizons on the order of thousands of timesteps. Because solution times for MINLPs scale poorly with the horizon length, we split the horizon into two linked contiguous parts of lengths N_1 and N_2, with $N_1 + N_2 = N$. We then approximate (1) by a problem where for the first N_1 steps we use the exact dynamics and constraints, while for the remaining N_2 steps we use linear approximations:

$$\min_{x,u} \sum_{t=0}^{N_1-1} g_t(x_t, u_t) + \sum_{t=N_1}^{N-1} \left(c_t^\top x_t + d_t^\top u_t\right) + c_N^\top x_N \tag{2a}$$

$$\text{s.t.} \quad x_{t+1} = \begin{cases} f_t(x_t, u_t), & t = 0, \ldots, N_1 - 1 \\ A_t x_t + B_t u_t, & t = N_1, \ldots, N-1 \end{cases} \tag{2b}$$

$$(u_t, x_t) \in \mathcal{Z}_t, \qquad t = 0, \ldots, N_1 - 1 \tag{2c}$$

$$E_t x_t + F_t u_t \leq h_t, \qquad t = N_1, \ldots, N-1 \tag{2d}$$

$$x_0 \text{ given.} \tag{2e}$$

For $t = 0, \ldots, N_1$, the costs, constraints, and dynamics of (2) are identical to those of (1). However, for $t = N_1, \ldots, N$, we have used linear approximations of f_t and g_t relative to problem (1), and added linear constraints (2d). The particular approximation method chosen should depend on the problem.

B. Split-Horizon Reformulation

To apply dynamic programming arguments, we rewrite the split-horizon problem (2) as two separate problems, linked by equating the terminal cost of the first horizon to the value function for the initial state of the second horizon.

The nonlinear first part of (2) can be written as

$$\min_{\substack{u_0,\ldots,u_{N_1-1} \\ x_1,\ldots,x_{N_1}}} \sum_{t=0}^{N_1-1} g_t(x_t, u_t) + V(x_{N_1}) \tag{3a}$$

$$\text{s.t.} \quad x_{t+1} = f_t(x_t, u_t), \quad t = 0, \ldots, N_1 - 1 \tag{3b}$$

$$(u_t, x_t) \in \mathcal{Z}_t, \qquad t = 0, \ldots, N_1 - 1 \tag{3c}$$

$$x_0 \text{ given.} \tag{3d}$$

The linear second part of (2) can be written as

$$V(x_{N_1}) = \min_{\substack{u_{N_1},\ldots,u_{N-1} \\ x_{N_1+1},\ldots,x_N}} \sum_{t=N_1}^{N-1} \left(c_t^\top x_t + d_t^\top u_t\right) + c_N^\top x_N \tag{4a}$$

$$\text{s.t.} \quad x_{t+1} = A_t x_t + B_t u_t, \tag{4b}$$

$$E_t x_t + F_t u_t \leq h_t, \tag{4c}$$

$$t = N_1, \ldots, N-1.$$

$$x_{N_1} \text{ given.} \tag{4d}$$

$V(x_{N_1})$ is a value function that encapsulates the optimal cost of (4), depending on the state x_{N_1}.

III. Solution of Split-Horizon Problem using DDP

A. Value Functions for LPs via DDP

It is difficult to solve (4) analytically as a function of parameter x_{N_1}, particularly for high state dimension. The conventional approach to dynamic programming (DP) would suggest calculating the value function over a grid of discrete states; the necessary calculation, however, scales exponentially in the dimension of the state space. DDP instead provides a piecewise-affine lower bound to the value as a function of the *continuous* state [1]. The construction is based on the following lemma.

Lemma 1: Given a solution to (4) for some $\hat{x}_{N_1}$, let $\hat{\lambda}$ and $\hat{\nu}$ be the dual variables corresponding to the constraints (4b) and (4c) at timestep $t = N_1$. Then, $\left(A_{N_1}^\top \hat{\lambda} + E_{N_1}^\top \hat{\nu} + c_{N_1}\right)^\top x_{N_1} - \hat{\nu}^\top h_{N_1}$ is a lower bound on $V(x_{N_1})$ for all x_{N_1}.

Proof: Given $\hat{x}_{N_1}$, (4) can be rewritten as the following primal problem, with $x_L = (x_{N_1+1}, \dots, x_N)$, $u_L = (u_{N_1}, \dots, u_{N-1})$, and A_L, B_L, c_L, d_L, E_L, F_L, and h_L defined correspondingly.

$$
\begin{aligned}
P(\hat{x}_{N_1}) = \min_{x_L, u_L} \quad & c_{N_1}^\top \hat{x}_{N_1} + c_L^\top x_L + d_L^\top u_L && \text{(5a)}\\
\text{s.t.} \quad & x_{N_1+1} = A_{N_1}\hat{x}_{N_1} + B_{N_1} u_{N_1}, && \text{(5b)}\\
& E_{N_1}\hat{x}_{N_1} + F_{N_1} u_{N_1} \le h_{N_1}, && \text{(5c)}\\
& A_L x_L + B_L u_L = 0, && \text{(5d)}\\
& E_L x_L + F_L u_L \le h_L, && \text{(5e)}\\
& \hat{x}_{N_1} \text{ given.} && \text{(5f)}
\end{aligned}
$$

Assigning the dual variables λ and ν to constraints (5b) and (5c), the partial Lagrangian of problem (5) is

$$
\begin{aligned}
L(x_L, u_L, \lambda, \nu) = {} & c_{N_1}^\top \hat{x}_{N_1} + c_L^\top x_L + d_L^\top u_L \\
& + \lambda^\top (A_{N_1}\hat{x}_{N_1} + B_{N_1}\overline{J} u_L - \overline{I} x_L) \\
& + \nu^\top (E_{N_1}\hat{x}_{N_1} + F_{N_1}\overline{J} u_L - h_{N_1}) \quad (6)
\end{aligned}
$$

where $\nu \ge 0$, $\overline{J} u_L = [I\ 0\ \dots\ 0] u_L = u_{N_1}$, and $\overline{I} x_L = [I\ 0\ \dots\ 0] x_L = x_{N_1+1}$.

The corresponding dual problem is

$$
D(\hat{x}_{N_1}) = \max_{\lambda, \nu} \ \left(c_{N_1}^\top + \lambda^\top A_{N_1} + \nu^\top E_{N_1}\right)\hat{x}_{N_1} - \nu^\top h_{N_1} \quad \text{(7a)}
$$

$$
\begin{aligned}
\text{s.t. } & d_L^\top + \lambda^\top B_{N_1}\overline{J} + \nu^\top F_{N_1}\overline{J} = 0, && \text{(7b)}\\
& c_L^\top - \lambda^\top \overline{I} = 0, && \text{(7c)}\\
& \nu \ge 0. && \text{(7d)}
\end{aligned}
$$

Now, consider the dual problem as an explicit function of x_{N_1}. If $\hat{\lambda}$ and $\hat{\nu}$ are the optimal arguments for (7) when $x_{N_1} = \hat{x}_{N_1}$, then they are also feasible for other choices of x_{N_1} since x_{N_1} does not enter the constraints of (7). However, they are in general only optimal for $\hat{x}_{N_1}$, and thus

$$
D(x_{N_1}) \ge \left(c_{N_1}^\top + \hat{\lambda}^\top A_{N_1} + \hat{\nu}^\top E_{N_1}\right) x_{N_1} - \hat{\nu}^\top h_{N_1}.
$$

Since strong duality holds for (5), $V(x_{N_1}) \equiv P(x_{N_1}) = D(x_{N_1})$. Thus, $\left(c_{N_1}^\top + \hat{\lambda}^\top A_{N_1} + \hat{\nu}^\top E_{N_1}\right) x_{N_1} - \hat{\nu}^\top h_{N_1}$ is a valid lower bound for $V(x_{N_1})$ over the entire state space. This inequality is tight for $x_{N_1} = \hat{x}_{N_1}$. ∎

Let $a = A_{N_1}^\top \hat{\lambda} + E_{N_1}^\top \hat{\nu} + c_{N_1}$ and $b = -\hat{\nu}^\top h_{N_1}$ be the parameters defining the linear lower bound of Lemma 1 arising from solving the problem for a particular $\hat{x}_{N_1}$. Solving the problem repeatedly for different $\hat{x}_{N_1}$ leads to a family of lower-bounding linear functions $\{a_1^\top x_{N_1} + b_1, \dots, a_j^\top x_{N_1} + b_j\}$. The individual lower bounds can be combined into an approximate value function

$$
\tilde{V}_j(x_{N_1}) = \max_{i=1,\dots,j} \ \{a_i^\top x_{N_1} + b_i\}, \quad (8)
$$

Algorithm 1 Split-horizon DDP with nonlinear first horizon

Data: cost function g_t for $t \in \{1, \dots, N\}$, system model
Result: u: optimal input

Initialize: $\{(a, b)\} = \emptyset$;
$j = 1$;
ϵ = desired solution tolerance ;
$UB = \epsilon$, $LB = -\epsilon$;

while $(UB - LB > \epsilon)$ **do**

1. Solve (3) using $\tilde{V}_j(x_{N_1}) = \max_{i=1,\dots,j} \{a_i^\top x_{N_1} + b_i\}$ as in (8). If $\{(a, b)\}$ is empty, then let $\tilde{V}_j(x_{N_1}) = 0$;
2. $LB = \sum_{t=0}^{N_1-1} g_t(x_t, u_t) + \tilde{V}_j(x_{N_1})$ using x, u from step 1 ;
3. Solve (4) using x_{N_1} from step 1 ;
4. Add $a_j = A_{N_1}^\top \lambda + E_{N_1}^\top \nu + c_{N_1}$ and $b_j = -\nu^\top h_{N_1}$ to collection of hyperplanes bounding $V(x_{N_1})$. Dual variables λ and ν found in step 3, correspond to (4b) and (4c) at $t = N_1$;
5. $UB = \sum_{t=0}^{N_1-1} g_t(x_t, u_t) + \sum_{t=N_1}^{N-1} \left(c_t^\top x_t + d_t^\top u_t\right) + c_N^\top x_N$, using x, u from steps 1 and 3 ;
6. $j = j + 1$;

end

which itself is a lower bound on the true value function $V(x_{N_1})$. The shape of $\tilde{V}_j$ depends on the points $\hat{x}_{N_1}$ that were used to generate the linear approximation, and the value is exact at those points. This is illustrated in Fig. 1.

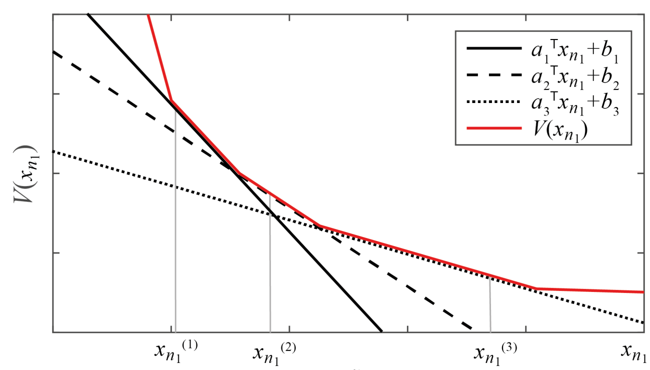

Fig. 1. Approximate value function $\tilde{V}_j(x_{n_1})$ calculated via DDP, as a function of state x_{n_1}. Hyperplanes found using DDP when computing a solution near a particular point are underestimates of the value function at all other points in the state space. $\tilde{V}_j(x_{n_1})$ is the pointwise maximum among the set of j lower-bound hyperplanes.

B. DDP Algorithm

We propose the DDP-like Algorithm 1 as an iterative approach to solving (2). Algorithm 1 constructs a collection of hyperplanes that forms a lower bound on the value function of the linear part (4) of the split-horizon problem, as a function of the state x_{N_1}. Each iteration of the algorithm introduces an additional hyperplane constraint at the current optimal x_{N_1}, thus providing a piecewise-linear approximation of $V(x_{N_1})$ which can be incorporated into (3). Since (3) is still a non-convex problem, to establish convergence we need to impose the following assumption.

Assumption 1: Given a piecewise-affine function $\tilde{V}_j(x_{N_1})$, the short-term nonlinear problem (3) with $\tilde{V}_j(x_{N_1})$ in place of $V(x_{N_1})$ can be solved to optimality.

We can now state the main result of this paper.

Theorem 1: Under Assumption 1, Algorithm 1 converges to the optimal solution of (2) in finitely many iterations.

Proof: Algorithm 1 additively constructs a set of underestimates of $V(x_{N_1})$, consisting of all (λ_j, ν_j) found when evaluating (7) at various x_{N_1}. Since (7) is a linear program, there are a finite number of distinct dual-feasible vertices (λ_j, ν_j), and an optimal solution must occur at one of these vertices. By Lemma 1, at iteration j, if $a_j = c_{N_1} + A_{N_1}^\top \lambda_j + E_{N_1}^\top \nu_j$ and $b_j = -\nu_j^\top h_{N_1}$, then $\tilde{V}_j(x_{N_1}) = \max_{i=1,\ldots,j} \{a_i^\top x_{N_1} + b_i\}$ is an underestimate of $V(x_{N_1})$. By Assumption 1, solving (3) using $\tilde{V}_j(x_{N_1})$ yields the following lower bound on (2):

$$LB = \sum_{t=0}^{N_1-1} g_t(x_t, u_t) + \tilde{V}_j(x_{N_1}).$$

By solving (5) using the $\hat{x}_{N_1}$ found in (3), we find feasible x_L and u_L, as well as the exact $V(x_{N_1})$ (since we are evaluating at $x_{N_1} = \hat{x}_{N_1}$). The resulting objective of (2),

$$\begin{aligned} UB &= \sum_{t=0}^{N_1-1} g_t(x_t, u_t) + c_{N_1}^\top x_{N_1} + c_L^\top x_L + d_L^\top u_L \\ &= \sum_{t=0}^{N_1-1} g_t(x_t, u_t) + V(x_{N_1}) \end{aligned}$$

is an upper bound on the cost of (2).

Suppose the lower and upper bounds are not equal. Then $\tilde{V}_j(x_{N_1}) < V(x_{N_1})$. Each time (5) is solved at a new $\hat{x}_{N_1}$, Algorithm 1 adds a new feasible vertex (λ_j,ν_j) to $\tilde{V}_j(x_{N_1})$, making the lower and upper bounds equal at this $\hat{x}_{N_1}$. Since there are a finite number of vertices to add, eventually we will have set the lower and upper bounds equal at the optimal x_{N_1}, and will thus reach the solution to (2). ■

Remark 1: The above proof does not require that the constraints or objective function in the short horizon be linear or convex. The only requirement on the problem is that of Assumption 1, namely that it be possible to solve the short-term nonlinear problem to global optimality.

IV. Application: Power-to-Gas Storage

We consider cost minimization for a large-scale power-to-gas plant exposed to spot electricity prices. Power-to-gas plants, which consist of electrolyzers, gas storage, and fuel cells, typically have round-trip efficiencies of 35% [11]. Despite the low efficiency, gas storage may still be a viable option in energy systems, as it is relatively cheap and expandable, and has low self-discharge over time. We use a model of a custom 100 kW power-to-gas plant under development by Paul Scherrer Institut in Villigen, Switzerland [12].

A. System Modeling Assumptions

Electrical energy is converted to hydrogen and oxygen gas using a proton electrolyte membrane (PEM) electrolyzer with a nonlinear conversion efficiency. The gas storage is modeled as a discrete-time integrator with continuous state, a storage capacity of 40m^3 hydrogen gas, and no self-discharge. Energy is converted back from gas to electricity using a PEM fuel cell, also with a nonlinear conversion efficiency [8]. Gas production and consumption as a function of device power is derived by fitting quadratic functions with zero constant terms to experimental data from the conversion devices. Both devices incur fixed power costs of 5% of their power limits (i.e., 5 kW) each timestep they are switched on.

We consider day-ahead hourly electricity spot market prices, which are settled for the following day at noon of the current day [13]. This results in a receding horizon optimal control problem with a decision block of 24 periods. Following [6], we assume deterministic prices as a best-case scenario and upper bound on the system performance.

B. Energy Storage Problem Formulation

The cost minimization problem for an energy storage device is written as a mixed integer quadratically-constrained program (MIQCP) over a horizon N. As in (3) and (4), we approximate the exact MIQCP as a split-horizon problem. The first, nonlinear subproblem of length $N_1 \leq N$ is

$$\min_{\substack{P^{\mathrm{C}}, P^{\mathrm{DC}} \\ \delta^{\mathrm{C}}, \delta^{\mathrm{DC}} \\ E^{\mathrm{C}}, E^{\mathrm{DC}}, x}} \sum_{t=0}^{N_1-1} p_t \left(P_t^{\mathrm{C}} + f^{\mathrm{C}}\delta_t^{\mathrm{C}} - P_t^{\mathrm{DC}} + f^{\mathrm{DC}}\delta_t^{\mathrm{DC}}\right) + V(x_{N_1}) \tag{9a}$$

$$\begin{aligned} \text{s.t.}\quad & x_{t+1} = x_t + E_t^{\mathrm{C}} - E_t^{\mathrm{DC}}, && (9b) \\ & E_t^{\mathrm{C}} = \alpha^{\mathrm{C}}(P_t^{\mathrm{C}})^2 + \beta^{\mathrm{C}} P_t^{\mathrm{C}}, && (9c) \\ & E_t^{\mathrm{DC}} = \alpha^{\mathrm{DC}}(P_t^{\mathrm{DC}})^2 + \beta^{\mathrm{DC}} P_t^{\mathrm{DC}}, && (9d) \\ & 0 \leq x_t \leq x_{\max}, && (9e) \\ & 0 \leq P_t^{\mathrm{C}} \leq P_{\max}^{\mathrm{C}} \delta_t^{\mathrm{C}}, && (9f) \\ & 0 \leq P_t^{\mathrm{DC}} \leq P_{\max}^{\mathrm{DC}} \delta_t^{\mathrm{DC}}, && (9g) \\ & \delta_t^{\mathrm{C}} \in \{0,1\},\ \delta_t^{\mathrm{DC}} \in \{0,1\}, && (9h) \\ & \quad t = 0, \ldots, N_1 - 1. && \\ & x_0 \text{ given.} && (9i) \end{aligned}$$

The second, linear subproblem is

$$\min_{\substack{P^{\mathrm{C}}, P^{\mathrm{DC}} \\ \delta^{\mathrm{C}}, \delta^{\mathrm{DC}} \\ E^{\mathrm{C}}, E^{\mathrm{DC}}, x}} \sum_{t=N_1}^{N-1} p_t \left(P_t^{\mathrm{C}} + f^{\mathrm{C}}\delta_t^{\mathrm{C}} - P_t^{\mathrm{DC}} + f^{\mathrm{DC}}\delta_t^{\mathrm{DC}}\right) - \bar{p} x_N \tag{10a}$$

$$\begin{aligned} \text{s.t.}\quad & x_{t+1} = x_t + E_t^{\mathrm{C}} - E_t^{\mathrm{DC}}, && (10b) \\ & E_t^{\mathrm{C}} \leq \gamma_i^{\mathrm{C}} P_t^{\mathrm{C}} + \eta_i^{\mathrm{C}} \quad \forall\, i = 1, \ldots, n^{\mathrm{C}} && (10c) \\ & E_t^{\mathrm{DC}} \geq \gamma_i^{\mathrm{DC}} P_t^{\mathrm{DC}} + \eta_i^{\mathrm{DC}} \quad \forall\, i = 1, \ldots, n^{\mathrm{DC}} && (10d) \\ & 0 \leq x_t \leq x_{\max}, && (10e) \\ & 0 \leq P_t^{\mathrm{C}} \leq P_{\max}^{\mathrm{C}} \delta_t^{\mathrm{C}}, && (10f) \\ & 0 \leq P_t^{\mathrm{DC}} \leq P_{\max}^{\mathrm{DC}} \delta_t^{\mathrm{DC}}, && (10g) \\ & 0 \leq \delta_t^{\mathrm{C}} \leq 1,\ 0 \leq \delta_t^{\mathrm{DC}} \leq 1 && (10h) \\ & \quad \forall\, t = N_1, \ldots, N. && \\ & x_{N_1} \text{ given.} && (10i) \end{aligned}$$

In the notation of the generic problem (2), the input is $u_t = (P_t^{\mathrm{C}},\ P_t^{\mathrm{DC}},\ \delta_t^{\mathrm{C}},\ \delta_t^{\mathrm{DC}},\ E_t^{\mathrm{C}},\ E_t^{\mathrm{DC}})$, and the state x_t is the volume of stored hydrogen. At each timestep t, the electrolyzer uses charging power P_t^{C} to store energy E_t^{C}, while the fuel cell discharges energy E_t^{DC} to produce power P_t^{DC}.

The exact quadratic system dynamics for the charged and discharged energy E_t^{C} and E_t^{DC} are used in (9). E_t^{C} is a concave quadratic function of P_t^{C}, i.e., $\alpha^{\mathrm{C}} \leq 0$ and $\beta^{\mathrm{C}} \geq 0$ in (9c). E_t^{DC} is a convex quadratic function of P_t^{DC}, i.e., $\alpha^{\mathrm{C}} \geq 0$ and $\beta^{\mathrm{C}} \geq 0$ in (9d). The exact conversion efficiency models are not published for these proprietary devices.

A piecewise-affine approximation of the system dynamics is used in (10). In (10c) and (10d), E_t^{C} and E_t^{DC} are given as epigraph variables over a set of n^{C} and n^{DC} affine approximations of the original quadratic curves [8]. Note that this method restricts us to piecewise-affine approximations that are concave for the charging device, and convex for the discharging device. In the case of negative prices, the inequalities for E_t^{C} will not be tight. By representing the problem in this manner, we implicitly allow for "spillage" to occur, where some of the charging power is wasted.

Each subproblem has a terminal cost. In (9a), the terminal cost $V(x_{N_1})$ represents the optimal value of (10) as a function of the storage at time N_1. In (10a), stored energy at the end of the horizon is valued at the mean energy price $\bar{p}$ over that horizon. This is done for simplicity, but the terminal cost could alternately incorporate the prices of electricity futures contracts, for example.

The first subproblem (9) has two sources of nonlinearity. First, a fixed per-period power usage of f^{C} and f^{DC} is incurred every time a charging or discharging device is run, resulting in binary variables δ_t^{C} and δ_t^{DC} for the device statuses (on or off). Second, while the storage device follows simple discrete-time integrator dynamics, the conversion efficiencies are quadratic.

V. Results and Discussion

To assess the optimality of the split-horizon method (3) and (4), we solve the problem using a fixed exactly-modeled horizon length. We apply the solution for the first day, and then re-solve for the subsequent horizon in a receding horizon manner. To allow for a comparison with other methods over a fixed horizon, the receding horizon shrinks over time. For example, for a problem horizon of 40 days, of which three are exactly modeled, the problem is solved as an MIQCP for the first three days, and a linear approximation for the following 37 days. The next step solves the three day MIQCP starting at the second of 40 days, followed by a linear approximation for the next 36 days, and so on.

A. Experimental Results over Short Horizons

We initially consider the exact MIQCP for horizon lengths over which we can compute the optimal solution. Fig. 2 illustrates the performance of the proposed split-horizon scheme over a horizon of 40 days starting on October 1, 2016, as a function of the length of the exact first part of the horizon. The problem, when solved over a receding horizon with three days of exact modeling, achieves 99.7% of the maximum profit available, while zero days of exact modeling (i.e., solving (10) over the entire horizon) achieves 95.4% of the optimum. This suggests that significant performance gains can be obtained by modeling a few days with high fidelity. The figure also illustrates the benefit of solving over a receding horizon, compared to projecting the initial split-horizon solution for the entire problem onto the feasible set of the exact nonlinear problem.

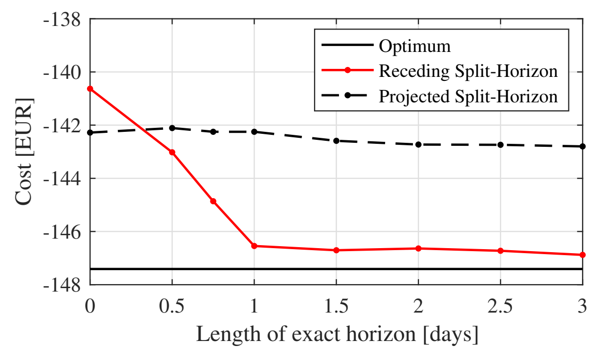

Fig. 2. Cost comparison of approximate solutions to a mixed integer quadratically-constrained linear program (MIQCP) over a horizon of 40 days starting on October 1, 2016. Negative costs are more optimal.

Prices are known exactly throughout the horizon; the only difference between the exact and split-horizon problems is in modeling the fixed costs and conversion efficiency over the second part of the horizon.

B. Computational Complexity of Split-Horizon Problem

Using Algorithm 1 to solve the split-horizon problem also has computational benefits. Fig. 3 illustrates the computational complexity of solving one instance of the split-horizon optimization problem (9) and (10) to convergence with a three day exact horizon. Two solution methods are presented. First, the split-horizon problem (9) and (10) is solved iteratively as in Algorithm 1. Second, the short and long horizons are combined into one horizon (analogous to (2)), and solved directly as a combined MIQCP. These two methods are compared to the complexity of solving the exact MIQCP for the entire horizon. As the total horizon length grows, the computation time for the exact MIQCP increases exponentially, while that of solving the split-horizon problem grows at a much slower rate. As illustrated, for sufficiently long horizons, the iterative method of Algorithm 1 is fastest.

The above problems were solved using Gurobi on an Intel i7-5820 3.30 GHz CPU with 16 GB RAM. The nonlinear MIQCPs were solved to the default optimality gap using the Gurobi branch-and-bound algorithm.

In Assumption 1, we required that the nonlinear short-term problem be solved to global optimality. Note that this holds in general for MIQCPs, but can also hold for other (low-dimensional) problems, using global optimization techniques such as spatial branch-and-bound algorithms [14].

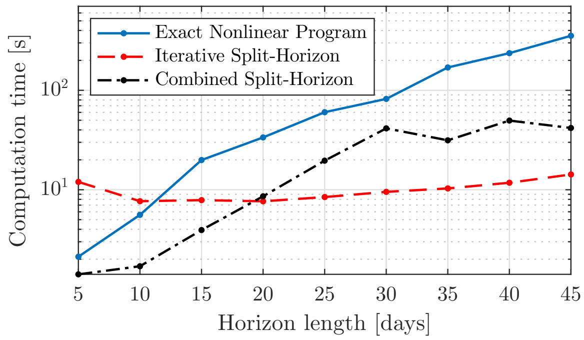

Fig. 3. Comparison of computation time of exact deterministic MIQCP, relative to that of split-horizon approximate problem with three day exact horizon. Computation time given as a function of total horizon (1 day = 24 hourly periods).

C. Horizons with Intractable Exact Model

As the proposed split-horizon method mainly targets long horizons which are affected by seasonal cycles, we solved the split-horizon problem over a total horizon of 365 days (365*24 = 8760 timesteps), with the first three days modeled exactly. For this total horizon length, problem (1) can no longer be solved exactly. Nevertheless, Fig. 4 shows that the split-horizon method with three days of exact horizon outperforms a linearized model by $\sim$3%. The split-horizon method implemented in a receding horizon also outperforms the initial solution projected onto the feasible set by $\sim$2.3%.

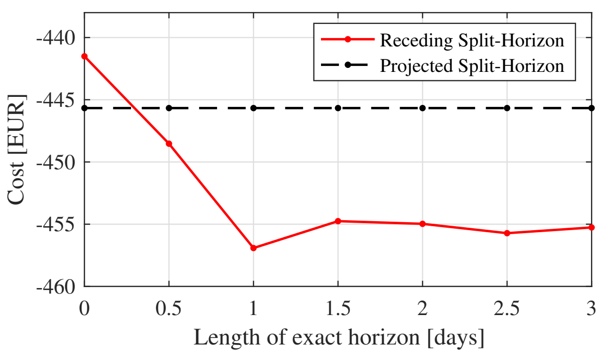

Fig. 4. Cost comparison of approximate solutions to MIQCP, over a shrinking horizon of 365 days starting on January 1, 2016.

VI. Conclusions and Extensions

We propose a split-horizon iterative method for solving discrete-time nonlinear optimal control problems over long horizons. We show that by having an accurate short-term model, and approximate long-term model, in a numerical example we achieve a more optimal solution over a longer time horizon than possible with either an accurate or simplified model. This is due to computational intractability and modeling inaccuracy respectively. By splitting the horizon in this manner, constraints that cannot be handled by regular DDP, like nonlinear dynamics and constraints over multiple timesteps, are respected by the chosen control actions. Furthermore, proceeding in a receding horizon manner reduces the impact of modeling inaccuracies in the long term.

This method can be applied to broader classes of long-term and large-scale stochastic problems, including the seasonal management of energy commodities like natural gas or ground heat storage, by adapting the formulation to account for stochasticity at each time step. For an energy storage device, potential sources of stochasticity include inflows, electricity prices, and energy demand. In the short nonlinear part of the horizon, a scenario approach can simulate high-dimensional stochastic models, allowing considerable flexibility in model complexity. In the longer linear part of the horizon, we can model stochastic processes as a recombining scenario tree [15]. In this case, hyperplanes generated by DDP at a given price state can be shared across all scenarios. The tractability and near-optimality of the split-horizon scheme allows for the inclusion of a larger number of scenarios, potentially improving control performance in a stochastic setting.

Acknowledgment

The authors would like to thank Roy Smith and members of the Paul Scherrer Institute's ESI project, especially Peter Jansohn and Christian Peter, for insightful discussions that inspired this work.

References

[1] M. V. F. Pereira and L. M. V. G. Pinto. "Multi-stage stochastic optimization applied to energy planning," Mathematical Programming, vol. 52, pp. 359–375, 1991.

[2] T. A. Rotting and A. Gjelsvik, "Stochastic dual dynamic programming for seasonal scheduling in the Norwegian power system," in IEEE Transactions on Power Systems, vol. 7, no. 1, pp. 273-279, Feb 1992.

[3] H. Abgottspon, K. Njálsson, M. A. Bucher, and G. Andersson, "Risk-averse medium-term hydro optimization considering provision of spinning reserves," 2014 International Conference on Probabilistic Methods Applied to Power Systems (PMAPS), Durham, 2014, pp. 1-6.

[4] S. Cerisola, J.M. Latorre, and A. Ramos. "Stochastic dual dynamic programming applied to nonconvex hydrothermal models," European Journal of Operational Research, 218(3), 687–697, 2012.

[5] N. Löhndorf, D. Wozabal, and S. Minner. "Optimizing Trading Decisions for Hydro Storage Systems Using Approximate Dual Dynamic Programming," in Operations Research, vol. 61, no. 4, pp. 810–823, January 2014.

[6] H. Abgottspon and G. Andersson. "Multi-horizon Modeling in Hydro Power Planning," Energy Procedia, 87, 2–10, 2016.

[7] S. Ahmed, A. J. King, and G. Parija. "A Multi-Stage Stochastic Integer Programming Approach for Capacity Expansion under Uncertainty," Journal of Global Optimization, 26(1), 3–24, 2003.

[8] P. Gabrielli, B. Flamm, A. Eichler, M. Gazzani, J. Lygeros, and M. Mazzotti, "Modeling for Optimal Operation of PEM Fuel Cells and Electrolyzers," in Environment and Electrical Engineering (EEEIC), 2016 IEEE 16th International Conference on. IEEE, 2016, pp. 1–7.

[9] F. Borelli, A. Bemporad, M. Morari. *Predictive control for linear and hybrid systems*. Cambridge University Press: Cambridge, UK, 2017.

[10] Bellman, Richard E. *Dynamic Programming*. Princeton N.J.: Princeton University Press, 1957.

[11] S.Walker, U. Mukherjee, M. Fowler, and A. Elkamel. "Benchmarking and selection of Power-to-Gas utilizing electrolytic hydrogen as an energy storage alternative," International Journal of Hydrogen Energy, vol. 41, no. 19, pp. 7717-7731, 2016.

[12] ESI Platform. https://www.psi.ch/media/esi-platform. Accessed Oct. 25, 2017.

[13] European Power Exchange Swiss Spot Market Price. https://www.epexspot.com/en. Accessed Oct. 25, 2017.

[14] E. M. B. Smith and C.C. Pantelides."A symbolic reformulation/spatial branch-and-bound algorithm for the global optimisation of nonconvex MINLPs," Computers and Chemical Engineering, vol. 23(4–5), pp.457–478, 1999.

[15] S. Rebennack. "Combining sampling-based and scenario-based nested Benders decomposition methods: application to stochastic dual dynamic programming," Mathematical Programming, vol. 156(1–2), pp.343–389, 2016.